Baleen whale navigation in astronomically referenced magnetic coordinates

Travis Horton

travis.horton@canterbury.ac.nz

University of Canterbury https://orcid.org/0000-0003-0558-2970

Nan Daeschler Hauser

Cook Islands Whale Research

Alexandre Zerbini

U.S. National Marine Mammal Laboratory

Daniel Palacios

Marine Mammal Institute, Oregon State University https://orcid.org/0000-0001-7069-7913

Audun Rikardsen

The Arctic University of Tromsø - UiT

Christian Lydersen

Norwegian Polar Insttute

Kit Kovacs

Norwegian Polar Institute

Mónica Silva

Universidade dos Açores https://orcid.org/0000-0002-2683-309X

Rui Prieto

University of the Azores

Rochelle Constantine

University of Auckland https://orcid.org/0000-0003-3260-539X

Leena Riekkola

Te Kura Mātauranga Koiora | School of Biological Sciences, Te Whare Takiura Mātai Pūtaiao Moana | Institute of Marine Science, Waipapa Taumata Rau | University of Auckland

Claire Garrigue

UMR ENTROPIE I- RD https://orcid.org/0000-0002-8117-3370

Solène Derville

UMR ENTROPIE (IRD, IFREMER, CNRS, Université de Nouvelle-Calédonie, Université de La Réunion)

Mads Peter Heide-Jørgensen

Greenland Institute of Natural Resources https://orcid.org/0000-0003-4846-7622

Michael C. Double

Australian Antarctic Division

Virginia Andrews-Goff
Australian Antarctic Division https://orcid.org/0000-0002-4609-7317
Nick Gales
Australian Antarctic Division
Yulia Ivashchenko
Seastar Scientific
Phillip Clapham
Seastar Scientific
Bruce Mate
Marine Mammal Institute, Oregon State University, Hatfield Marine Science Center

---

Biological Sciences - Article

Keywords:

Posted Date: July 1st, 2024

DOI: https://doi.org/10.21203/rs.3.rs-4613940/v1

Additional Declarations: There is **NO** Competing Interest.

Baleen whale navigation in astronomically referenced magnetic coordinates

Travis W. Horton[1], Nan Hauser[2], Alexandre N. Zerbini[3], Daniel M. Palacios[4*], Audun H. Rikardsen[5], Christian Lydersen[6], Kit M. Kovacs[6], Mónica A. Silva[7], Rui Prieto[7], Rochelle Constantine[8], Leena Riekkola[8], Claire Garrigue[9], Solène Derville[9], Mads P. Heide-Jorgensen[10], Michael C. Double[11], Virginia Andrews-Goff[11], Nicholas J. Gales[11], Yula V. Ivashchenko[12], Phillip J. Clapham[12], Bruce R. Mate[4]

Affiliations:

1-Te Kura Aronukurangi | School of Earth and Environment, University of Canterbury, Private Box 4800, Christchurch 8041, New Zealand (travis.horton@canterbury.ac.nz)

2 – Cook Islands Whale Research, Center for Cetacean Research and Conservation, P.O. Box 3069, Avarua, Rarotonga, Cook Islands, South Pacific (nan@whaleresearch.org)

3 - Cooperative Institute for Climate, Ocean, & Ecosystem Studies**,** John M. Wallace Hall, 3737 Brooklyn Ave NE, Seattle, WA 98105 (alex.zerbini@noaa.gov)

4- Marine Mammal Institute, Oregon State University, Hatfield Marine Science Center, 2030 SE Marine Science Dr, Newport, Oregon 97365, USA (daniel.palacios@oregonstate.edu; bruce.mate@oregonstate.edu; bruce.mate@oregonastate.edu)

5 – UiT The Arctic University of Norway, Faculty of Bioscience, Fisheries and Economics, 9037 Tromsø, Norway (audun.rikardsen@uit.no)

6 - Norwegian Polar Institute, Fram Center, Tromsø, Norway (christian.lydersen@npolar.no; kit.kovacs@npolar.no)

7 - Okeanos – Instituto de Investigação em Ciências do Mar, University of the Azores, Rua Prof Frederico Machado, 4, 9901-862 Horta Portugal (monica.silva.imar@gmail.com; rcabprieto@gmail.com)

8 - Te Kura Mātauranga Koiora | School of Biological Sciences, Te Whare Takiura Mātai Pūtaiao Moana | Institute of Marine Science, Waipapa Taumata Rau | University of Auckland, Tāmaki Makaurau | Auckland, Aotearoa | New Zealand (r.constantine@auckland.ac.nz; lrie003@aucklanduni.ac.nz)

9 – UMR ENTROPIE (IRD, IFREMER, CNRS, Université de Nouvelle-Calédonie, Université de La Réunion), Nouméa 98800, New Caledonia (Claire.garrigue@ird.fr; solene.derville@ird.fr)

10 – Greenland Institute of Natural Resources, Box 570, Nuuk, DK-3900, Greenland (mhj@ghsdk.dk)

11 – Australian Marine Mammal Centre, Australian Antarctic Division, 203 Channel Highway, Kingston, TAS 7050, Australia

12 - Seastar Scientific, Vashon, WA, USA (phillip.clapham@gmail.com)

* - Current affiliation: Center for Coastal Studies, 5 Holway Avenue, Provincetown, Massachusetts, 02657, USA

Abstract

How animals navigate during long-distance migration remains a mystery. Many theories have been proposed[1] (Keeton, 1979), with the Earth's magnetic field emerging as a clear potential source of orientational information for navigational decision-making across diverse taxa[2] (Putman, 2022). Yet, the mechanics involved in magnetic navigation remain unknown[3] (Schneider et al., 2023). Globally distributed records available from historic whaling[4-5] (AOWLD, 2023; Yablokov et al., 1998) in combination with modern satellite-tracking datasets[6] (Horton et al., 2022) for baleen whales create a unique opportunity to illuminate the mechanics of cetacean navigation. Here, we show that baleen whale migratory destinations over the last >200 years are systematically distributed in horizontal plane magnetic coordinates. Specifically, blue (*Balaenoptera musculus*), bowhead (*Balaena mysticetus*), fin (*Balaenoptera physalus*), gray (*Eschrichtius robustus*), humpback (*Megaptera novaeangliae*), and right (*Eubalaena* spp.) whales non-randomly inhabit areas where magnetic declination (MD) closely approximates integer and half-integer multiples of the Earth's 23.44° axial tilt. Our findings, which are highly reproducible through both space and time, demonstrate that baleen whale navigation between seasonal habitats occurs via the integration of magnetic and astronomic orientation cues[3]. By referencing MD values to the rise and set azimuths of the Sun, baleen whale movements define mechanistic horizontal plane heliomagnetic coordinate trajectories across all ocean basins.

Main

The migratory behaviour of baleen whales has fascinated people for centuries, and we have learned a considerable amount about their remarkable journeys around the planet through dedicated observation, acoustic monitoring and tracking[6] (Horton et al., 2022). Traditional Māori knowledge describes trans-oceanic ancestral human migrations that were guided by whales[7] (Lythberg and Ngata, 2022), and modern satellite-tracking confirms that migratory corridors of some species have been stable over prolonged periods[8] (Horton et al., 2020). In addition, many whales unerringly return year after year to highly specific locations on feeding grounds[9] (Clapham et al., 1993). However, we now also know that baleen whale movements exhibit notable variability[10-11] (Kennedy et al., 2014a; Reisinger et al., 2021), including large differences in seasonal habitat selection despite using the same migratory corridors[12-13] (Bailey et al., 2009; Riekkola et al., 2019), and surprising examples of apparent vagrancy[14] (Hoelzel et al., 2021), as well as recolonization[15] (Herr et al., 2022) of former habitats following recoveries from whaling. Centuries of experience and observation provide a reasonable understanding of when and where many baleen whale species go during their long-distance migrations, and global datasets are now large enough to turn our attention to illuminating mechanistically how baleen whales navigate between seasonal habitats with such remarkable fidelity[16] (Horton et al., 2017).

Over two-hundred years of digitized historic whaling-ship logbooks[4-5] (AOWLD, 2023; Yablakov et al., 1998) make baleen whales one of the few clades where multi-centennial analyses of distribution possible at the global scale. The widespread deployment of satellite tags on a wide variety of baleen whale species[6] (Horton et al., 2022) in combination with the whaling-ship archives creates an unprecedented opportunity to identify recurrent and reproducible non-random patterns in baleen whale distributions from a variety of orientational perspectives. In parallel, recent advances in magnetic modeling enable analyses of both main field and bedrock parameters over the past 1,000 years anywhere on the planet[17] (Schanner et al., 2023). As a consequence, the magnetic cues experienced by individual whales on specific dates and locations can now be quantified. Recognising these opportunities, we pursued the integration of American[4] (AOWLD, 2023) and Soviet[5,18] (Yablakov et al., 1998; Tormosov, pers. comm.) whaling-ship logbook archives and satellite-tracking locations using modern magnetic[17,19-20] (NCEI, 2017; Chulliat et al., 2020; Schanner et al., 2023) and astronomical models[21] (Meeus, 1991) to determine whether or not baleen whale distribution data from the past ~240 years follow mechanistic patterns across Earth's magnetic field.

Using published geographic coordinate Gregorian calendar location data derived from baleen whale satellite-monitored platform transmitting terminal (PTT) data[6,8,10-13,22-52], we determined the magnetic declinations experienced by 280 blue whales, 80 fin whales, 12 gray whales, 666 humpback whales, 49 right whales and 68 bowhead whales (Table 1; Extended Data Table 1). To quantify the most commonly experienced magnetic declination (MD) values, we analysed these data using kernel density estimation (KDE). MD distributions were non-random (G test; $p<<0.05$) and multimodal, reflecting the widely distributed seasonal habitats deliberately selected by these migratory whales (Table 1).

Table 1. Magnetic declination distribution modes for baleen whales tracked using satellites.

Baleen Whale			**Modern Era Satellite Tracking**								
Genus	**Species**	**Common Name**	**Ocean Basin(s)**	**Number of Whales**	**Years (CE)**	**Number of Days**	**Major Mode: Magnetic Declination (°)**	**1st Minor Mode: Magnetic Declination (°)**	**2nd Minor Mode: Magnetic Declination (°)**	**3rd Minor Mode: Magnetic Declination (°)**	**References**
Megaptera	*novaeangliae*	Humpback Whale	North Pacific	262	1995 to 2020	6852	16.04	**9.75**	**24.72**	**1.23**	22-24
			South Pacific	154	2003 to 2018	7487	**13.55**	**47.51**	**35.35**	**-0.41**	8, 16, 25-29
			North Atlantic	11	2005 to 2019	886	-14.88	**-12.34**	**10.67**	17.72	30-31
			South Atlantic	162	2002 to 2019	5130	**-23.59**	-15.36	**-11.44**	-4.99	8, 32-33
			Indian	77	2014 to 2017	3210	**-0.66**	**-23.86**	-28.02	**-70.24**	11
			All	666	1995 to 2019	23565	15.70	**-23.68**	**9.97**	**-0.77**	8, 11, 16, 22-33
					Corresponding Locations:		Northwestern U.S.A.; Antarctic Peninsula	Abrolhos Bank, Brazil; Western South Africa	Hawai'i; Baja California Sur	Western Australia; Western South America	
Balaenoptera	*musculus*	Blue Whale	North Pacific	254	1993 to 2018	14530	**12.81**	**10.12**	5.71	3.50	12, 34-37
			South Pacific	11	2013 to 2016	488	8.98	4.84	**11.61**	**1.13**	38
			North Atlantic	15	2009 to 2016	383	**-9.90**	**-11.94**	-14.17	-16.21	39
			South Atlantic	0	n.a.	n.a.	n.a.	n.a.	n.a.	n.a.	
			Indian	0	n.a.	n.a.	n.a.	n.a.	n.a.	n.a.	
			All	280	1993 to 2018	15401	**12.75**	9.59	5.38	**-9.93**	12, 34-39
					Corresponding Locations:		Offshore California; Offshore Chile	Offshore Mexico; Golfo de Corcovado, Chile	Costa Rica Dome; Svalbard	Azores; Jan Mayen	
Balaenoptera	*physalus*	Fin Whale	North Pacific	32	2002 to 2018	1559	**13.41**	18.20	20.77	n.a.	36, 40
			South Pacific	0	n.a.	n.a.	n.a.	n.a.	n.a.	n.a.	
			North Atlantic	48	2003 to 2019	1256	**-10.61**	**0.06**	-8.82	8.76	39, 41-43
			South Atlantic	0	n.a.	n.a.	n.a.	n.a.	n.a.	n.a.	
			Indian	0	n.a.	n.a.	n.a.	n.a.	n.a.	n.a.	
			All	80	2002 to 2019	2815	**13.23**	**-10.16**	**-0.06**	-4.74	36, 39-43
					Corresponding Location(s):		Offshore California; Svalbard	Azores; Jan Mayen	Northwestern Mediterranean Sea	Northeastern Atlantic	
Eschrichtius	*robustus*	Gray Whale	North Pacific	12	2010 to 2013	956	**-11.39**	**10.04**	14.93	-6.28	44-45
					Corresponding Location(s):		Northeastern Sakhalin Island, Sea of Okhotsk	Baja California Coast; Bering & Chukchi Seas	California Coast; Gulf of Alaska	Southeastern Kamchatka Peninsula	
Eubalaena	*japonica*	North Pacific Right Whale	North Pacific	0	n.a.	n.a.	n.a.	n.a.	n.a.	n.a.	
	australis	Southern Right Whale	South Pacific	0	n.a.	n.a.	n.a.	n.a.	n.a.	n.a.	
	glacialis	North Atlantic Right Whale	North Atlantic	16	1989 to 2000	356	-18.75	-14.16	-5.52	**-10.87**	46-48
	australis	Southern Right Whale	South Atlantic	33	2001 to 2017	2309	**1.84**	**-24.41**	**-22.56**	-6.81	49-50
	australis	Southern Right Whale	Indian	0	n.a.	n.a.	n.a.	n.a.	n.a.	n.a.	
		Right Whale	All	49	1989 to 2017	2665	**1.84**	**-24.41**	**-22.56**	-18.71	46-50
					Corresponding Locations:		Golfo Nuevo; Golfo San Matias; Coastal Argentina	Coastal South Africa; Eastern South Atlantic	West Coast South Africa; Central South Atlantic	Gulf of Maine; Central North Atlantic	
Balaena	*mysticetus*	Bowhead Whale	Arctic Ocean	68	1992 to 2017	6857	**-23.95**	-39.48	**36.16**	n.a.	51-52
					Corresponding Location(s):		Foxe Basin ; Gulf of Boothia	Northern Baffin Island Coast	Southern Beaufort Sea		
			Total:	**1155**	**1989 to 2019**	**52,259**					

Bold-faced numbers indicate modes in magnetic declination data distributions that occur within ±2° of integer, or half-integer, multiples of Earth's 23.44° axial tilt.

Initially, we considered the MD distributions of humpback whales satellite-tagged in different ocean basins, including the North Atlantic, South Atlantic, North Pacific, South Pacific and Indian Oceans (Table 1; Extended Data Figure 1). Our goal in this step was to develop a data-based hypothesis using modern satellite tracking data for the most widely studied species.

We discovered that humpback whales disproportionately inhabited sites where MD values consistently reflected integer and half-integer multiples of Earth's axial tilt (i.e., 23.44˚) irrespective of which ocean basin they used (Table 1; Extended Data Figure 1). Of the 20 major and minor modes identified in the compiled Atlantic, Indian and Pacific Ocean humpback whale satellite-tracking datasets (Table 1; Extended Data Figure 1), 70% occurred within ±2° of an integer or half-integer multiple of Earth's axial tilt ($p=0.00092$; Binomial Probability) and 50% occurred within ±1°($p=0.0006$; Binomial Probability). For example, humpback whales satellite-tagged in the South Atlantic most commonly occurred at -23.59˚, while the highest density MD value for Indian Ocean humpbacks was -0.66˚ (Table 1; Extended Data Figure 1). In total, three of five major modes, and 11 of 15 minor modes, in tagged humpback whale MD distributions, analysed at the ocean basin scale, are within ±2˚ of integer or half-integer multiples of the Earth's 23.44˚ axial tilt (Table 1; Extended Data Figure 1).

From a geographic perspective, the major and minor modes identified for humpback whale MD distributions correspond with well known breeding grounds, feeding areas, or stop-over locations (Table 1). Based on this initial empirical analysis, we hypothesized that other species of baleen whale would also disproportionately inhabit sites where MD values are within ±2.00˚ of integer and half-integer multiples of Earth's 23.44˚ axial tilt.

Our analyses on additional species support this hypothesis. Specifically, 17 of 34 major and minor modes in MD distributions for satellite-tagged blue, fin, gray, right and bowhead whales, identified using KDE, occur within ±2.00˚ of an integer or half-integer multiple of Earth's 23.44˚ axial tilt (p=0.0223, Binomial Probability; Table 1; Fig. 1; Extended Data Figure 2). These sites

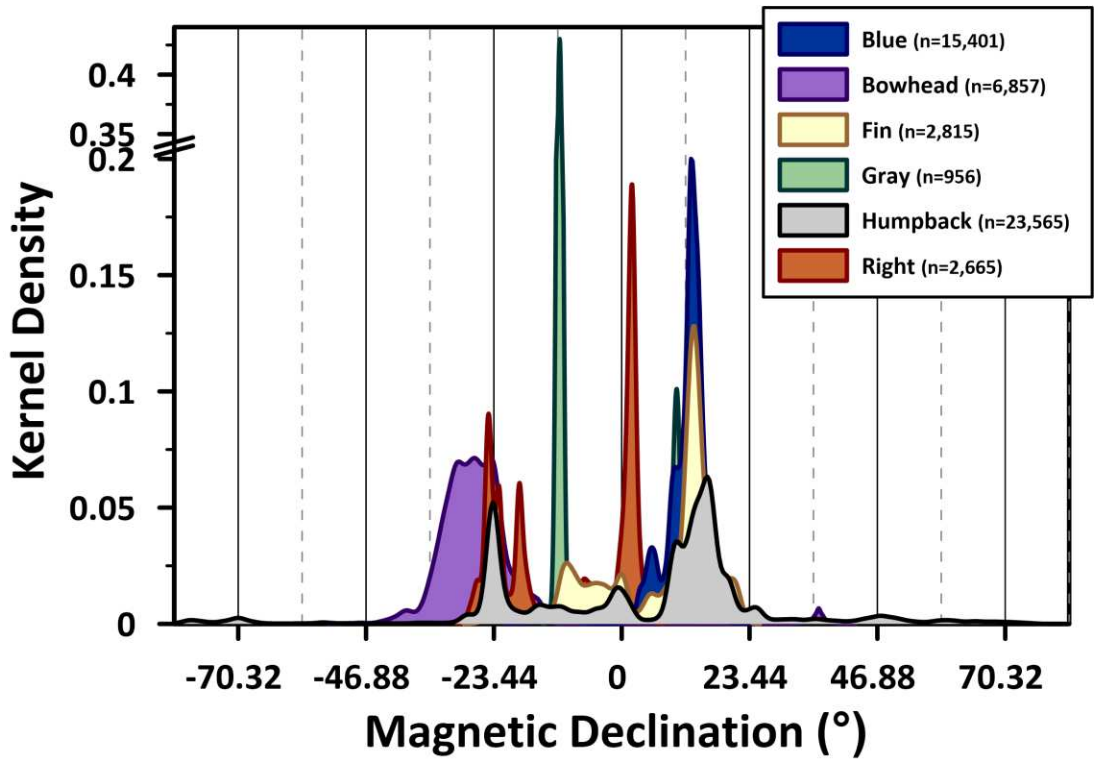

Fig. 1. Magnetic declination data distributions, determined by kernel density estimation, for satellite-tagged baleen whales. Colours, and the total number of once-daily platform transmitting terminal locations, as indicated in the legend.

correspond with seasonal baleen whale hot-spots, including the western North American coast, the Azores, Sea of Okhotsk, Foxe Basin, coastal Argentina, western Australia and the Antarctic Peninsula. Blue whales, fin whales and gray whales, satellite-tagged in the North Atlantic and North Pacific Oceans, non-randomly concentrated in areas where MD was within ±2° of 11.72° or -11.72°, while southern right whales (*Eubalaena australis*) disproportionately used areas where magnetic declination was within ±2.00˚ of 0˚ (e.g., coastal Argentina) or -23.44˚ (e.g., west coast South Africa). Despite their proximity to the northern hemisphere's magnetic pole, and their close association with sea ice, satellite-tagged bowhead whales also concentrated in areas where MD was within ±2.00˚ of -23.44° (e.g., Foxe Basin and Gulf of Boothia) and 35.16˚ (e.g., southern Beaufort Sea).

In total, 31 of 54 major and minor modes in satellite-tagged baleen whale MD distributions occur within ±2.00˚ of integer and half-integer multiples of 23.44˚ (Table 1; Fig. 1; Extended Data Figure 2). Binomial probability demonstrates that this recurrent pattern is extremely unlikely to have occurred due to random chance (p=0.00025, Binomial Probability). However, the magnetic field changes via secular variation, raising questions regarding whether or not such patterned distributions persist through time[53] (Alerstam, 2006). For example, secular variation causes MD values to change by <0.2° per year in most places and as much as 20° per year near the magnetic poles.

Analysis of >39,000 baleen whale locations, recorded in American and Soviet whaling-ship logbooks between 1784 and 1975 (Table 2; Fig. 2; Extended Data Table 2; Extended Data Figure 3), reinforces the pattern observed in the satellite-tracking dataset (Table 1; Fig. 1). Major and minor modes in logbook MD data distributions occur within ±2.00˚ of 0°, ±11.72°, ±23.44˚, -35.16°, or ±46.88° for: 1) humpback whales and blue whales in all but the South Pacific Ocean; 2) fin whales in all but the Indian Ocean; 3) gray whales in the North Pacific Ocean; 4) right whales in the Pacific, Atlantic and Indian Oceans; 5) bowhead whales in the Arctic Ocean (Table 2).

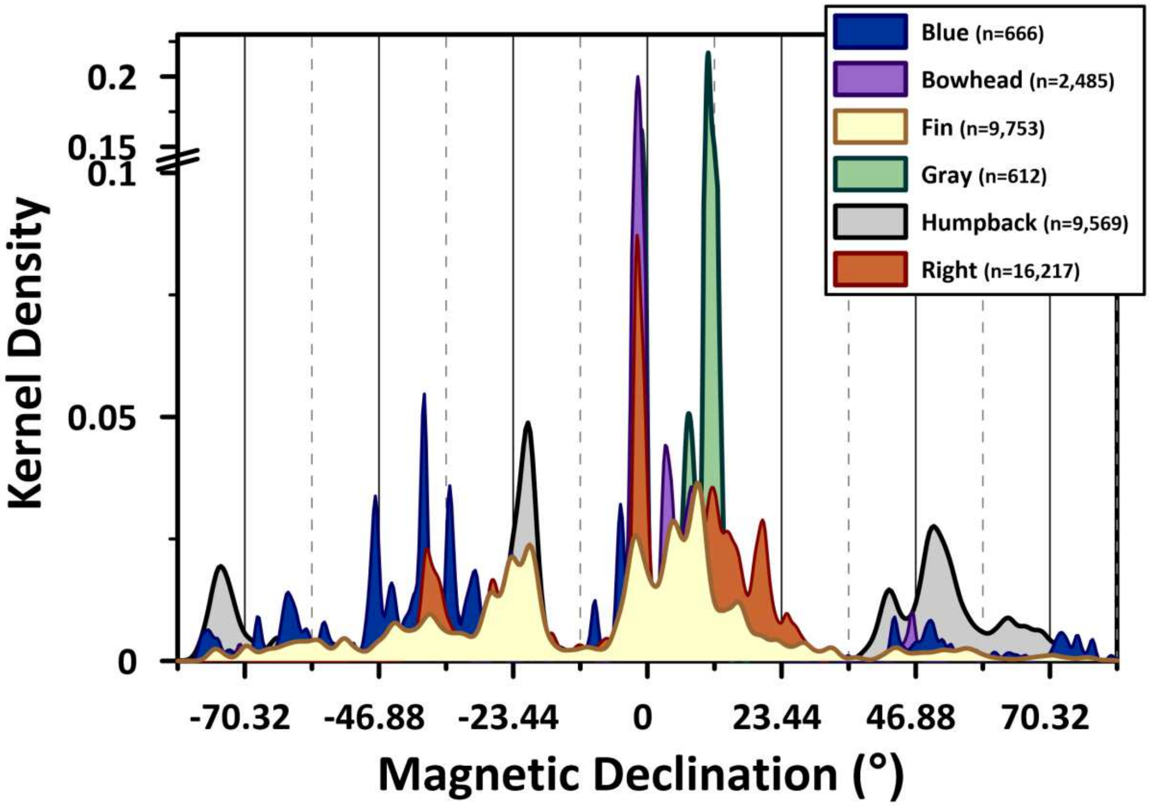

Fig. 2. Magnetic declination data distributions, determined by kernel density estimation, for historic American and Soviet whaleship logbook entries for baleen whales (colours as indicated in the legend). The total number of 'sights and strikes' for each species are indicated in the legend.

In total, 36 of 87 major and minor modes indentified in American and Soviet whale ship logbook MD data distributions occurred within ±2.00˚ of integer and half-integer multiples of Earth's 23.44˚ axial tilt (p=0.0322, Binomial Probability; Table 2). The slightly higher, but still significant, probability that whale- shiplogbook MD modes approximate integer and half-integer multiples of Earth's axial tilt likely reflects the lower precision of whale ship logbook latitude and longitude entries in comparison to satellite-tracking location data and greater uncertainty in palaeomagnetic models across large ocean basins like the South Pacific.

Table 2. Magnetic declination distribution modes for baleen whales struck or sighted during historic whaling.

Baleen Whale			Historic American & Soviet Whaling							
Genus	**Species**	**Common Name**	**Ocean Basin(s)**	**Years (CE)**	**Number of Strikes & Sightings**	**Major Mode: Magnetic Declination (°)**	**1st Minor Mode: Magnetic Declination (°)**	**2nd Minor Mode: Magnetic Declination (°)**	**3rd Minor Mode: Magnetic Declination (°)**	**References**
Megaptera	*novaeangliae*	Humpback Whale	North Pacific	1819 to 1893	565	**10.19**	5.33	**-0.63**	2.35	4
			South Pacific	1818 to 1972	4254	49.45	42.15	17.59	4.76	4-5, 18
			North Atlantic	1792 to 1902	376	-19.24	**0.42**	**-23.23**	**-12.07**	4
			South Atlantic	1815 to 1973	2525	-20.73	**-23.20**	-27.05	**13.62**	4-5, 18
			Indian	1792 to 1968	1849	-74.92	-64.60	**1.34**	**-48.78**	4-5, 18
			All	1792 to 1973	9569	-20.87	50.04	-74.52	5.00	4-5, 18
					Corresponding Location(s):	Southern South Atlantic; Abrolhos Bank	Balleny Islands; Southern Ocean - North of Amundsen Sea	Davis Sea	Equatorial West Coast, South America	
Balaenoptera	*musculus*	Blue Whale	North Pacific	1844 to 1893	90	-4.69	**10.86**	-2.46		4
			South Pacific	1844 to 1972	105	43.22	49.58	5.14	14.34	4-5, 18
			North Atlantic	1835 to 1895	21	-19.76	**-21.64**	**-23.80**	**-11.72**	4
			South Atlantic	1838 to 1973	104	**-23.80**	-20.32	-9.24	-30.11	4-5, 18
			Indian	1844 to 1969	346	-39.10	**-34.50**	**-47.45**	-2.21	4-5, 18
			All	1835 to 1973	666	-38.97	-2.16	**-34.55**	**-47.57**	4-5, 18
					Corresponding Location(s):	Azores; Crozet Islands	Southwest Coast of Australia; Sea of Japan	Lazarev Sea	Kerguelen Islands	
Balaenoptera	*physalus*	Fin Whale	North Pacific	1819 to 1893	892	**-0.22**	**-1.74**	4.26	-4.77	4
			South Pacific	1819 to 1975	1846	4.28	13.91	15.96	**10.28**	4-5, 18
			North Atlantic	1784 to 1916	622	**-24.49**	**-21.80**	-19.23	**-35.92**	4
			South Atlantic	1815 to 1975	4144	9.00	-20.54	**-23.84**	-27.41	4-5, 18
			Indian	1792 to 1969	2249	-2.25	-37.83	-44.12	-52.97	4-5, 18
			All	1784 to 1975	9753	8.88	4.04	-2.43	-20.50	4-5
					Corresponding Location(s):	Falkland Islands; Scotia Sea	Galapagos Islands; Tropical Eastern Pacific; Bering Sea	Orkney Islands; Sea of Okhotsk; West Coast of Australia	Southern South Atlantic	
Eschrichtius	*robustus*	Gray Whale	North Pacific	1845 to 1885	612	**10.63**	**-1.09**	7.23	n.a.	4
					Corresponding Location(s):	Baja California Sur	Sea of Okhotsk	Chukchi Sea		
Eubalaena	*japonica*	North Pacific Right Whale	North Pacific	1822 to 1904	7080	**-1.78**	**11.32**	8.86	3.87	4
	australis	Southern Right Whale	South Pacific	1797 to 1907	2495	20.05	**24.45**	13.97	9.51	4
	glacialis	North Atlantic Right Whale	North Atlantic	1838 to 1897	13	-48.97	-51.28	6.82	**-0.18**	4
	australis	Southern Right Whale	South Atlantic	1793 to 1968	3620	-27.13	**-36.85**	15.78	**-1.72**	4-5, 18
	australis	Southern Right Whale	Indian	1792 to 1967	3009	-38.59	-21.15	**-23.94**	**0.98**	4-5, 18
		Right Whale	All	1792 to 1968	16217	**-1.81**	**11.31**	20.12	-38.57	4-5, 18
					Corresponding Location(s):	Sea of Okhotsk; Sea of Japan; Central South Atlantic	Gulf of Alaska	Coast of Chile; Coast of Argentina; Louisville Ridge	Crozet Islands	
Balaena	*mysticetus*	Bowhead Whale	Arctic Ocean	1844 to 1912	2485	**-1.67**	3.12	20.67	**46.21**	4
					Corresponding Location(s):	Sea of Okhotsk	Bering Sea	Barrow, Alaska; Chukchi Sea	Beaufort Sea	
			Total:	**1784 to 1975**	**39,302**					

Bold-faced numbers indicate modes in magnetic declination data distributions that occur within ±2° of integer, or half-integer, multiples of Earth's 23.44° axial tilt.

Our analyses reveal that a similar pattern is present in both satellite-tracking and whaling archival data when analysed at the global scale (Fig. 1; Fig. 2). Of 141 major and minor modes identified in globally distributed blue, bowhead, fin, gray, humpback and right whale satellite-tracking and whaling-ship logbook MD data distributions (Table 1; Table 2, Fig. 1; Fig. 2; Extended Data Figure 2; Extended Data Figure 3), 67 (48%) are within ±2.00˚ of integer and half-integer multiples of 23.44˚ ($p=0.00032$, Binomial Probability). This recurrent non-random pattern in baleen whale habitat distribution demonstrates that baleen whales integrate horizontal plane magnetic and astronomic orientation cues during navigation.

Horizontal Plane Heliomagnetic Navigation

The data distributions we report raise the question: How do they do it? How do diverse whale populations, in all ocean basins across a >240 year period, integrate magnetic and astronomic orientation cues[54] (Wiltschko and Wiltschko, 2023)? The most salient answer involves the Sun.

The Sun provides potential spatiotemporal orientation cues via light-dark cycles and its position at rise, culmination and set[55] (Åkesson et al., 2014). These cues vary systematically and predictably across annual cycles as the Earth moves along its orbit, providing tangible oriential cues such as photoperiod, sunrise azimuth, culmination angle and sunset azimuth across most of the Earth's surface (Fig. 3). By convention, the horizontal plane cues sunrise azimuth, sunset azimuth and MD are quantified relative to a geographic north (i.e., 0°) direction (Fig. 3). However, this geocentric system of measurement does not preclude the possibility that baleen whales reference astronomic orientation cues relative to the position of the local magnetic field (e.g., SSA-MD), or vice versa.

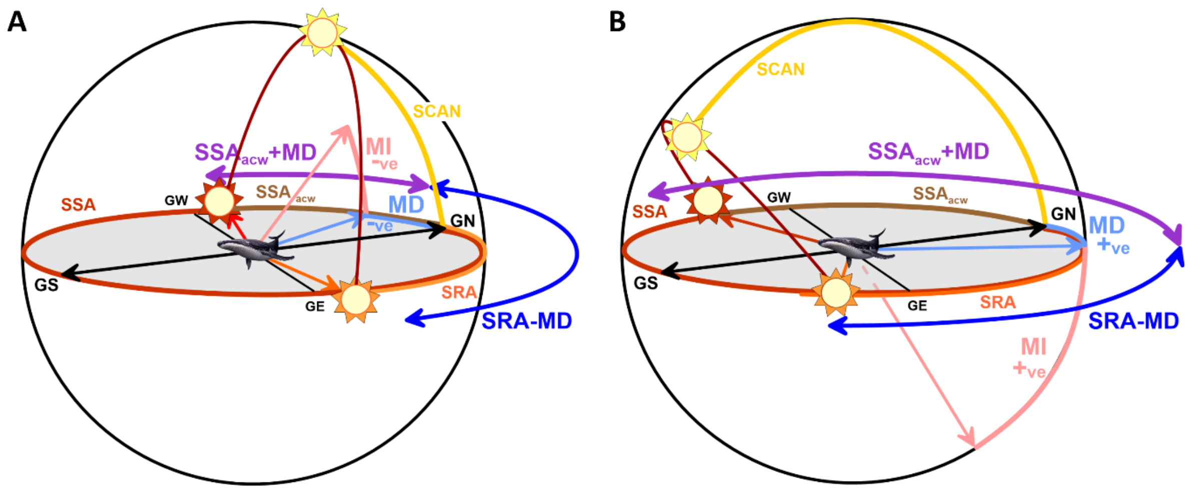

Fig. 3. Heliologic, magnetic and heliomagnetic orientation cues available to baleen whales in the southern (A) and northern (B) magnetic hemispheres. Abbreviations and colours are as follows: SRA = sunrise azimuth (orange), positive in the clockwise direction viewed from above; SSA = sunset azimuth (red), positive in the clockwise direction viewed from above; SSA_{acw} = sunset azimuth anti-clockwise (brown), positive in the anti-clockwise direction viewed from above; SCAN = sun culmination angular altitude relative to geographic north horizon (yellow); MD = magnetic declination (light blue), positive to the east of geographic north and negative to the west of geographic north; MI = magnetic inclination (pink), positive below the geographic north horizon and negative above the geographic north horizon. GN, GE, GS, and GW indicate the geographic north, east, south and west directions, respectively. Heliomagnetic coordinates, SRA-MD (blue) and SSA_{acw}+MD (purple), correspond with the angle in the horizontal plane between MD and SRA, and SSA_{acw}, respectively.

Such an integrated system of navigation has distinct advantages. When and where they occur, sunrise and sunset provide obvious light-dark temporal markers and potential orientation information via sun azimuth at sunrise (SRA) and sun azimuth at sunset (SSA). Such astronomic cues are highly structured and cyclical over the Earth's annual orbit. For example, at the equator, SRA and SSA move through a 46.88° (i.e., 2 x 23.44°) range centered on the east-west direction in the horizontal plane during each annual cycle. At the tropics (i.e., ±23.44° latitude) and polar circles (i.e., ±66.56°, or 90° - 23.44°, latitude), SRA and SSA move through 58° to 59° (i.e., ~2.5 x 23.44°) and 162° to 164° (i.e., ~7 x 23.44°) ranges, respectively. These highly patterned spatiotemporal cycles are the consequence of the Earth's 23.44° axial obliquity, the driver of the Earth's seasons. In addition to providing a seasonal - to annual - orientational framework, using the Sun as a reference point removes the organism's need to identify, and potentially remember, the direction of geographic north when sensing MD.

Other celestial bodies also follow sub-annual, annual and longer-term astronomic cycles, most notably the Moon[56] (Andreatta and Tessmar-Raible, 2020), but for the purposes of our study, we focus on the rise and set positions of the Sun. Thus, our analysis centers on two horizontal plane heliomagnetic coordinates: 1) the angle between SRA and MD (i.e., SRA-MD; Fig. 3), and 2) the angle between SSA, measured in an anti-clockwise direction (SSA_{acw}), and MD (i.e., SSA_{acw}+MD; Fig. 3).

When referenced relative to the rise and set positions of the Sun, the heliomagnetic locations of baleen whale migratory destinations and migration routes demonstrate many similarities

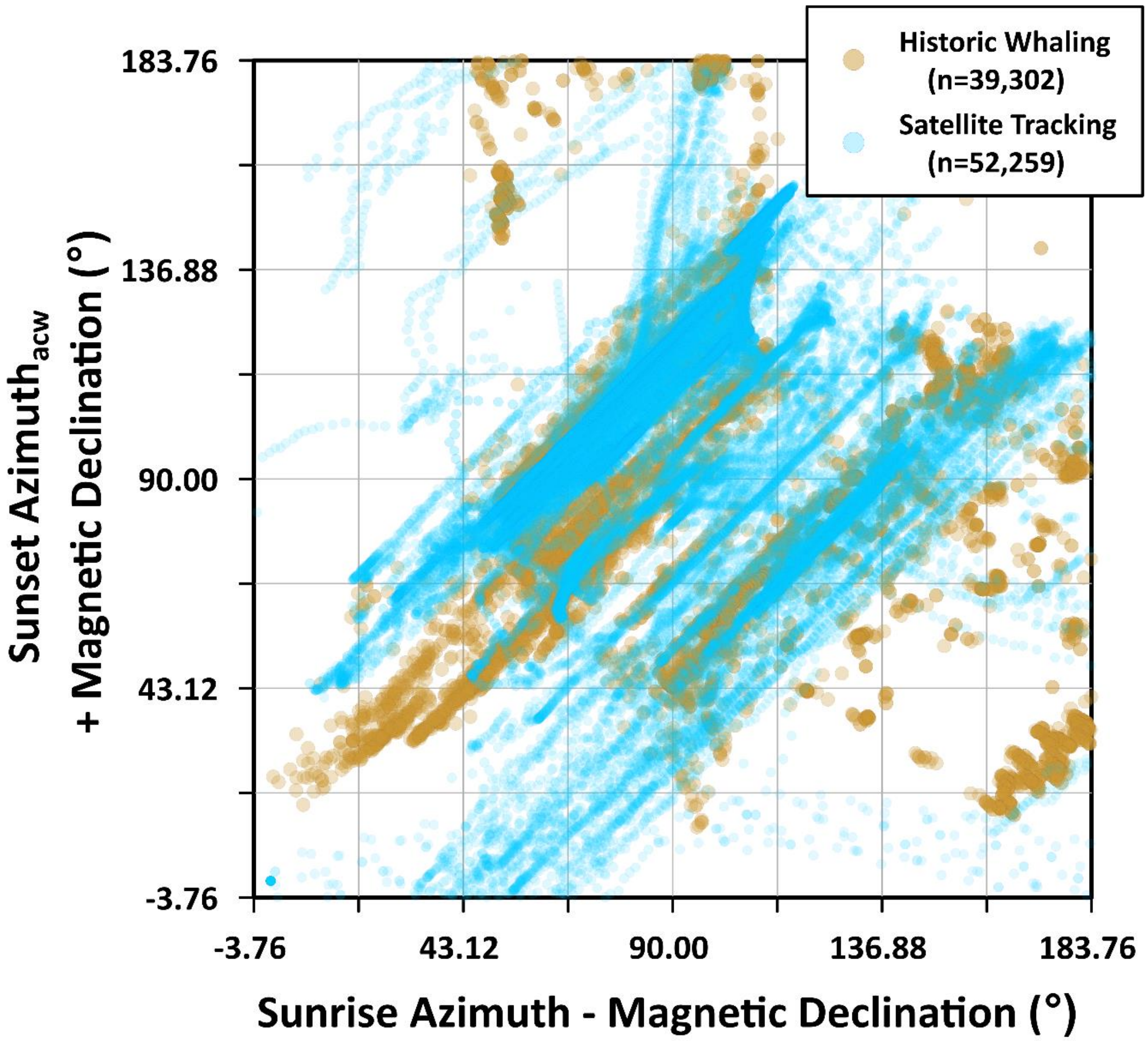

Fig. 4. Bivariate plot of sunset azimuth anti-clockwise plus magnetic declination (i.e., SSA_{acw}+MD) versus sunrise azimuth minus magnetic declination (i.e., SRA-MD) for historic American and Soviet whaling-ship logbook entries (brown circles) and satellite-tagged baleen whales (light blue circles).

irrespective of time, species or geographic location. For example, both historic whaling and modern satellite-tracking datasets include high-density 1:1 covariation trends between SRA-MD and SSA_{acw}+MD (Fig. 3; Fig. 4), corresponding with sites where MD closely approximates integer or half-integer multiples of Earth's axial tilt (Fig.1, Fig. 2, Fig. 4; Extended Data Figure 1). The strong 1:1 covariation between SRA-MD and SSA_{acw}+MD recognized in both the whaling and satellite-tracking datasets is a consequence of baleen whale seasonal residence (R) in areas where the difference between SRA-MD and SSA_{acw}+MD approximates an integer or half-integer multiple of Earth's obliquity through time:

$$(SRA - MD) - (SSA_{acw} + MD) \approx n \times 23.44°$$

where, n is an integer or half-integer.

The satellite-tracking dataset further reveals how individuals migrate between sites where MD approximates integer or half-integer multiples of 23.44° (Fig. 5). Three different navigational modes, which we introduce here as horizontal plane heliomagnetic navigation modes 1-3 (i.e., HH1, HH2, HH3), are apparent. The first heliomagnetic navigation mode, type 1 (i.e., HH1; Fig. 5A) , includes migration along a trajectory that follows an isogonic where MD closely approximates an integer or half-integer multiple of Earth's obliquity:

$$MD \approx n \times 23.44°$$

where, n is an integer or half-integer.

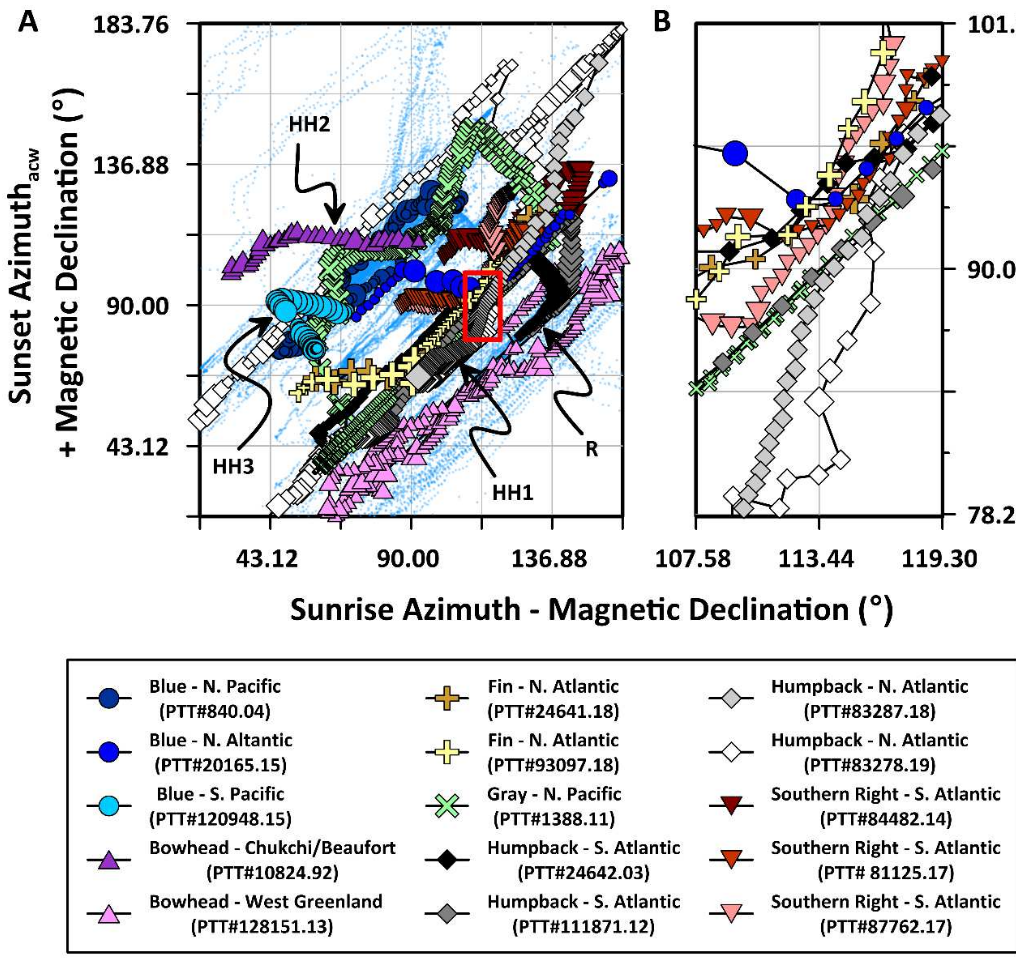

Fig. 5. Bivariate plot of sunset azimuth anti-clockwise plus magnetic declination (i.e., SSA_{acw}+MD) versus sunrise azimuth minus magnetic declination (i.e., SRA-MD) for satellite-tagged baleen whales. Red inset box in (A) is expanded in (B). Fifteen representative individual whales, tracked via satellite, are shown in (A) and are symbolized as indicated in the legend. Symbol sizes in (A) and (B) correspond with whale movement velocity. Examples of the three heliomagnetic navigation modes (HH1-HH3), and seasonal residence (R), described in the text are indicated via arrows. All other satellite tagging data is shown as small light blue circles in (A).

Since SRA and SSA_{acw} are typically within ±2.00° of each other on the same day of the year, depending on date and latitude, HH1 navigation causes strong 1:1 covariation between SRA-MD and SSA_{acw}+MD. In both residence (R) and HH1 modes, MD is effectively constant due to the whale's lack of movement (R) or movement along an isogonic (HH1). Thus, both residence and HH1 navigation cause strong 1:1 covariation between SRA-MD and SSA_{acw}+MD, with the key difference being the individual is actively migrating during HH1 navigation rather than remaining stationary.

There are many examples of HH1 navigation in the satellite-tracking dataset. For example, South Atlantic humpback whale PTT#111871.12 maintains MD within ±0.69° (±1σ) of -23.43°, during the first 22 days, and 2185 km, of its poleward migration in 2012 (Fig. 5A). Like many other whales in the dataset, PTT#111871.12 is able to navigationally maintain a MD value that is not significantly different (two-tailed t-test; $p>0.05$) than the MD value present in the seasonal habitat where it was satellite-tagged. Similarly, North Atlantic humpback whale PTT#83278.19 maintains MD within ±2.38° (±1σ) of -12.07° during the first 61 days, and 7388 km, of its poleward migration in 2019 (Fig. 5A). This MD value is not dissimilar (two-tailed t-test; $p>0.05$) to the MD value at its low latitude seasonable habitat in the Caribbean. By migrating along trajectories that maintain a 1:1 relationship between SRA-MD and SSA_{acw}+MD (i.e., HH1 navigation; Fig. 5A), baleen whales are able to maintain, during long-distance migration, the MD value present on their seasonal habitats with remarkable precision.

Type 2 horizontal plane heliomagnetic navigation (HH2) includes migration along trajectories that maintain near-constant integer or half-integer multiples of Earth's obliquity centered on a 90° angle. HH2 navigation occurs in either of the heliomagnetic coordinates, SRA-MD (HH2a) *or* SSA_{acw}+MD (HH2b), according to:

$$SRA - MD \approx (n \times 23.44°) + 90°$$

or,

$$SSA_{acw} + MD \approx (n \times 23.44°) + 90°$$

where, n is an integer or half-integer.

The satellite-tracking dataset includes many examples of HH2b navigation, but fewer examples of HH2a navigation. For example, South Pacific blue whale PTT#120948.15 maintains SSA_{acw}+MD within ±1.67° (±1σ) of 89.72° during the first 17 days, and 1584 km, of its west-soutwestward migration away from the Chilean coast despite ~10° changes in both SSA_{acw} and MD (Fig. 5). Similarly, Bering-Chukchi-Beaufort bowhead whale PTT#10824.92 maintains SSA_{acw}+MD within ±1.12° (±1σ) of 112.87° during the first 23 days, and 1651 km, of its westward migration across the Beaufort and Chukchi Seas despite experiencing ~26° changes in both SSA and MD (Fig. 5). North Atlantic fin whale PTT#24641.18's SSA_{acw}+MD location stays within ±2.00° (±1σ) of 66.57° during the first 7 days, and 759 km, of its southwestward migration away from Svalbard (Fig. 5), despite experiencing 15-20° changes in both MD and SSA over the same period, while South Atlantic southern right whale PTT#81125.17 maintains

SSA_{acw}+MD within ±0.42° (±1σ) of 91.88° during the first 25 days, and 1165 km, of its northeastward migration away from Peninsula Valdes (Fig. 5) despite ~12° changes in both SSA and MD.

Importantly, the satellite-tracking dataset demonstrates that some individuals switch between HH2a and HH2b navigational modes (Fig. 5). For example, South Atlantic southern right whale PTT#87762.17 maintains SSA_{acw}+MD (HH2b) within ±1.06° (±1σ) of 89.47° during the first 19 days, and 1261 km, of its initial northeasterly migration, followed by a 26 day period when it switched to maintain SRA-MD (HH2a) within ±1.36° (±1σ) of 116.33° across a 1174 km southwesterly movement, despite ~12° changes in both MD and SRA. Three years earlier, South Atlantic southern right whale PTT#84482.14 maintained a similar pattern with SSA_{acw}+MD being within ±0.90° (±1σ) of 111.00° (HH2b) during the first 21 days, and 1394 km, of its initially easterly migration away from Peninsula Valdes, immediately prior to a 4 day period when it switched to maintain SRA-MD within ±0.24° (±1σ) of 125.79° (HH2a) across the subsequent 400 km southerly leg of its migration. In all examples, HH2a-HH2b switching corresponds with prominent changes in geographic coordinate migration paths.

Type 3 horizontal plane heliomagnetic navigation (HH3), the least common in the dataset we analysed, includes migration along trajectories that maintain a -1:1 negative covariation between sequential heliomagnetic coordinate locations, according to:

$$SSA_{acw} + MD \approx -1(SRA - MD) + ((n \times 23.44°) + 180°)$$

where, n is an integer or half-integer.

An example of this type of navigation was performed by gray whale PTT#1388.11, that maintained a highly significant -1.09:1 negative covariation between SRA-MD and SSA_{acw}+MD (r^2=0.98; n=29; regression t-test; p<0.05; df=27; s.e.=0.027; m=-1.088) during its rapid 28 day, 4545 km, eastward migration across the North Pacific Ocean in December, 2011 (Fig. 5A). In the Southeast Pacific, blue whale PTT#120948.15 similarly maintained a highly significant -1.28:1 negative covariation (r^2=0.99; n=30; regression t-test; p<0.05; df=28, s.e.=0.0195; m=-1.284;) during its May-June, 2015, 4661 km, northward migration (Fig. 5A).

Notably, South Atlantic humpback whale PTT#24642.03 switched from HH1 navigation to HH3 navigation on 1 January, 2004, approximately 6 days into its southeastward migration. At first, PTT#24642.03 maintained MD within ±0.07° (±1σ) of -23.04° (i.e., HH1 navigation), during the first six days, and 697 km, of its migration away from Abrolhos Bank. Then the whale switched, doing a pronounced turn to the south-southwest, and shifting into HH3 navigation, whereafter, it maintained a highly significant -1.21:1 negative covariation (r^2=0.97; n=19; regression t-test; p<0.05; df=17, s.e.=0.0541; m=-1.208) during the remaining 34 days, and 3050 km, of its poleward migration (Fig. 5A).

The horizontal plane heliomagnetic trajectories followed by baleen whales (Fig. 5) provide insight into how integrated astronomic and magnetic cues facilitate long-distance return migration without compromising the ecological needs of the individual. Incorporation of astronomic cues, like the rise and set azimuths of the Sun, provide stable and seasonally structured orientation information, while using the position of the Sun as a reference datum for horizontal plane magnetic orientation overcomes the challenges associated with determining the direction of geographic north. Similarly, the potential orientational impacts of magnetic secular variation are also diminished through utilisation of an orbitally structured, and thus temporally cyclic, astronomic rather than geocentric reference frame.

Navigation in a spatiotemporally dynamic, but richly structured and rigidly cyclical, reference frame helps baleen whales locate and re-locate seasonal habitats at ecologically appropriate times of the year. For example, 19 whales converge on heliomagnetic moments when SRA-MD is within ±3° of 113.44° (i.e., 90° + 23.44°) and SSA_{acw}+MD is within ±3° of 90°, irrespective of species, ocean basin, date and navigational mode (Fig. 5B). Specifically, gray whale PTT#1388.11 and humpback whale PTT#111871.12 passed through this heliomagnetic waypoint while residing in Sea of Okhotsk and South Atlantic Ocean feeding areas, respectively. In contrast, southern right whales, PTT#81125.17 and PTT#87762.17, converged on this node at the northeastern-most point of their seasonal migrations away from Peninsula Valdes, while fin whale, PTT#24641.18, arrived at this node following ~1000 km of swimming away from Svalbard and immediately prior to a 22-day migratory stop-over near Jan Mayen, ~600 km north of Iceland. In the North Atlantic and South Atlantic, humpback whales, PTT#83728.19 and PTT#24642.03, converged on this node at the start, and end, of their annual long-distance migrations, respectively (Fig. 5B). These examples demonstrate that baleen whales are capable of navigating to, and changing their movement behaviours at, specific nodes, or navigational waypoints, in heliomagnetic coordinates that are closely associated with the 23.44° obliquity of Earth’s axis of rotation.

There appear to be many heliomagnetic coordinate waypoints, associated with integer and half-integer multiples of Earth’s obliquity, that baleen whales converge on. For example, baleen whales disproportionately converge on any combination of heliomagnetic coordinate moments when and where SRA-MD and SSA_{acw}+MD are within ±3° of 66.56° (i.e., 90.00° - 23.44°), 90.00° and 113.44° (i.e., 90.00°+23.44°; Extended Data Figure 4). Thus, the data we report suggest that, in addition to providing a rigid orbitally-tuned structure, the integration of astronomic and magnetic cues during navigation also provides flexibility via the cyclical symmetry of heliomagnetic waypoints across the annual cycle. Such flexibility not only helps whales successfully navigate between established habitats, but also provides a spatiotemporal system through which habitat can be (re)colonized and explored. Such examples include the return of fin whales to Elephant Island[15] (Herr et al., 2022) and gray whales to Hawaiian waters[50], and gray whale vagrancy into the Atlantic[14] (Hoelzel et al., 2021)(Extended Data Figure 4).

Summary

Using historical American and Soviet whaling-ship archives and modern satellite-tracking datasets, we demonstrate that baleen whales navigate using horizontal plane magnetic coordinates referenced relative to astronomic cues, including the rise and set positions of the sun. This conclusion is supported by several lines of evidence including the non-random occurrence of major and minor modes in baleen whale magnetic declination data distributions near integer and half-integer multiples of Earth's axial obliquity. When referenced relative to the azimuth of the sun at rise and set, these horizontal plane magnetic coordinates are reframed as heliomagnetic coordinates, and become a function of both space and time.

Our analyses show that over the past ~240 years baleen whales have disproportionately inhabited sites where heliomagnetic coordinates describe highly significant covariant trends that intersect integer and half-integer multiples of Earth's obliquity centered on 90° right angles. We recognise three different recurrent modes of heliomagnetic navigation across species and ocean basins, including migration along specific isogonics, prolonged maintenance of specific heliomagnetic coordinate values, and movements that describe highly significant negative covariation trends in heliomagnetic coordinates through space and time. Furhermore, our analysis reveals that integrated astronomic and magnetic cues serve as spatially and temporally dynamic orientational waypoints for whales migrating between habitats at ecologically favourable times of the year. Such mechanistic understanding of baleen whale navigation and associated movement decisions is important due to increasing human-whale interactions in a rapidly changing global environment impacted by anthropogenic development and climate change. Identifying the drivers of periodicities in baleen whale movements facilitates predictions of when and where humans and whales may come into conflict and how whales will be impacted by environmental change.

Many questions emerge from this research. Are similar patterns present in vertical plane heliomagnetic coordinates? Do other organismal clades utilise a similar system of navigation? Can the times and locations of seasonal residence and migration be accurately predicted? How are magnetic and astronomic cues sensed, transduced and integrated? Answering these questions requires both analysis of existing animal tracking and experimental orientation datasets as well as future experiments on model organisms specifically designed to elucidate which cues are integrated, and which are not, during different movement behaviours.

Methods

Geographic coordinate Gregorian calendar baleen whale satellite-monitored platform transmitting terminal (PTT) locations were compiled from published sources (Table 1). The Argos Data Collection and Location System used for this project (http://www.argos-system.org/) is operated by Collecte Localisation Satellites. Argos is an international program that relies on instruments provided by the French Space Agency flown on polar-orbiting satellites operated by the U.S. National Oceanic and Atmospheric Administration, the European Organisation for the Exploitation of Meteorological Satellites, and the Indian Space Research Organization.

Once-daily whale locations, limited to dates when Argos-derived PTT messages were received, were interpolated from velocity filtered (<20 km h^{-1}) Argos messages using Paleontological Statistics software[58]. American[4] and Soviet[5,18] whaleship logbook locations were used as reported and were not interpolated. Harvest data associated with Soviet whaling (i.e., species, latitude, longitude, date, time), came from a dataset of 51,746 catches by the factory fleet *Yuri Dolgorukiy*, which operated in the Southern Hemisphere between 1960 and 1975, and were kindly provided by Dr. Dmitry Tormosov (Kaliningrad, Russia)[18]. Magnetic field elements, including declination, inclination, and flux density (i.e., field intensity), were determined from latitude, longitude, and decimal year using the World Magnetic Model[20], the Enhanced Magnetic Model 2017[19], and the HistKalMag[17] models. Rise and set azimuths of the Sun at baleen whale locations were determined using astronomical algorithms[21].

Magnetic declination data distributions were determined using kernel density estimation[59-60]. Binomial probability was used to determine the probability that KDE major and minor modes would occur within ±2° of integer and half-integer multiples of 23.44° based on a 34.13% (i.e., 8 ÷ 23.44) chance of success. The probability that observed magnetic declination KDE data distributions would result from random chance alone was determined using the G test, also known as the log likelihood ratio test[61], using oceanic magnetic declination data, determined for a 1° latitude/longitude global grid, as the expected random magnetic declination data distribution. Two-tailed regression t-tests were used to determine whether or not significant linear relationships exist between SRA-MD and SSA_{acw}+MD in the satellite-tracking data of individual whales.

Acknowledgements

This study would not have been possible without the hard work and support of many individuals, including all of those who contributed to the satellite-tracking and whaling-ship logbook digitisation. We are immensely grateful for your commitment and contributions. T.W.H. thanks the University of Canterbury for a 2023 sabbatical grant-in-aid and the Brian Mason Science and Technical Trust for supporting this research. N.H. thanks the University of Canterbury for a Sustainable Development Goals Doctoral Scholarship. The original version of the manuscript was greatly improved by constructive reviews and feedback from anonymous referees.

Author Contributions

T.W.H. and N.H. conceived the study, performed all original magnetic, astronomical and statistical data analyses, prepared the table and figures, and drafted the initial manuscript. All authors compiled the published satellite-tracking datasets and helped revise the manuscript.

Additional Information

Competing interests. The authors declare no competing interests.

Supplementary Information is available for this paper.

Correspondence and requests for materials should be addressed to Travis Horton (travis.horton@canterbury.ac.nz).

How to cite this article: Horton, T.W. *et al.* Baleen whale navigation in astronomically referenced magnetic coordinates. (2024)

Terminology

culmination – the time at which the Sun passes the local meridian (*syn:* meridian transit).

heliomagnetic – from the Greek helios (i.e., Sun) and Latin magneta (i.e., relating to magnetism), meaning of, or pertaining to, the association between the Sun and magnetism.

isogonic – path connecting points on the surface of the Earth whereat magnetic declination is the same.

kernel density estimation – nonparametric model for estimating the probability distribution of a dataset; in this study, the Gaussian kernel function (i.e., $k(x) = \frac{1}{\sqrt{2\pi}} e^{\frac{-1}{2}x^2}$ was used.

magnetic declination – angle in the horizontal plane between the local magnetic field and geographic north reckoned positive to the east and negative to the west.

major mode – highest local maximum in a multimodal data distribution.

minor modes – sequentially lower frequency local maxima, following the major mode, in a multimodal data distribution.

obliquity – angle between an object's rotational axis and its orbital axis (*syn:* axial tilt). Earth's obliquity ranges between ~22.1° and ~24.5° across an ~41,000 year cycle and is currently ~23.436°.

recolonisation – in biology, the repopulation of previously occupied habitat.

secular variation (*magnetism*) – change in the intensity and shape of Earth's magnetic field through time.

sunrise azimuth – direction of the Sun, when the upper edge of the Sun's climbing disk passes the horizontal, measured relative to geographic north and reckoned clockwise positive.

sunset azimuth – direction of the Sun, when the upper edge of the Sun's falling disk passes the horizontal, measured relative to geographic north and reckoned clockwise positive. In this study, the subscript ‘acw’ indicates sunset azimuth reckoned anti-clockwise positive (i.e., 360° - sunset azimuth).

vagrancy – occurrence of an animal well outside its normal range.

waypoint – a set of coordinates that identifies a specific location along a route of travel (*syn:* node).

References

1 - Keeton, W.T., 1979. Avian orientation and navigation. *Annual Review of Physiology*, *41*(1), pp.353-366.

2 - Putman, N.F., 2022. Magnetosensation. *Journal of Comparative Physiology A*, *208*(1), pp.1-7.

3 - Schneider, W.T., Packmor, F., Lindecke, O. and Holland, R.A., 2023. Sense of doubt: inaccurate and alternate locations of virtual magnetic displacements may give a distorted view of animal magnetoreception ability. *Communications Biology*, *6*(1), p.187.

4 - American Offshore Whaling Logbook Data, https://whalinghistory.org, Mystic Seaport Museum, Inc. and New Bedford Whaling Museum. Accessed [12 January, 2023]

5 - Yablokov, A.V., Zemsky, V.A., Mikhalev, Y.A., Tormosov, V.V. and Berzin, A.A., 1998. Data on Soviet whaling in the Antarctic in 1947-1972 (population aspects). *Russian Journal of Ecology*, *29*(1), pp.38-42.

6 - Horton, T.W., Palacios, D.M., Stafford, K.M. and Zerbini, A.N., 2022. Baleen Whale Migration. In *Ethology and Behavioral Ecology of Mysticetes* (pp. 71-104). Cham: Springer International Publishing.

7 - Lythberg, B. and Ngata, W., 2022. Heeding the Call of Paikea. *Across Species and Cultures*, p.245.

8 - Horton, T.W., Zerbini, A.N., Andriolo, A., Danilewicz, D. and Sucunza, F., 2020. Multi-decadal humpback whale migratory route fidelity despite oceanographic and geomagnetic change. *Frontiers in Marine Science*, p.414.

9 - Clapham, P.J., Baraff, L.S., Carlson, C.A., Christian, M.A., Mattila, D.K., Mayo, C.A., Murphy, M.A. & Pittman, S. 1993. Seasonal occurrence and annual return of humpback whales in the southern Gulf of Maine. *Canadian Journal of Zoology* 71: 440-443.

10 - Kennedy, A.S., Zerbini, A.N., Rone, B.K. and Clapham, P.J., 2014a. Individual variation in movements of satellite-tracked humpback whales *Megaptera novaeangliae* in the eastern Aleutian Islands and Bering Sea. *Endangered Species Research*, *23*(2), pp.187-195.

11 – Reisinger, R.R., Friedlaender, A.S., Zerbini, A.N., Palacios, D.M., Andrews-Goff, V., Dalla Rosa, L., Double, M., Findlay, K., Garrigue, C., How, J. and Jenner, C., 2021. Combining regional habitat selection models for large-scale prediction: Circumpolar habitat selection of Southern Ocean humpback whales. *Remote Sensing*, *13*(11), p.2074.

12 - Bailey, H., Mate, B.R., Palacios, D.M., Irvine, L., Bograd, S.J. and Costa, D.P., 2009. Behavioural estimation of blue whale movements in the Northeast Pacific from state-space model analysis of satellite tracks. *Endangered Species Research*, *10*, pp.93-106.

13 – Riekkola, L., Andrews-Goff, V., Friedlaender, A., Constantine, R. and Zerbini, A.N., 2019. Environmental drivers of humpback whale foraging behavior in the remote Southern Ocean. *Journal of experimental marine biology and ecology*, *517*, pp.1-12.

14 - Hoelzel, A.R., Sarigol, F., Gridley, T. and Elwen, S.H., 2021. Natal origin of Namibian grey whale implies new distance record for in-water migration. *Biology Letters*, *17*(6), p.20210136.

15 - Herr, H., Viquerat, S., Devas, F., Lees, A., Wells, L., Gregory, B., Giffords, T., Beecham, D. and Meyer, B., 2022. Return of large fin whale feeding aggregations to historical whaling grounds in the Southern Ocean. *Scientific Reports*, *12*(1), p.9458.

16 - Horton, T.W., Hauser, N., Zerbini, A.N., Francis, M.P., Domeier, M.L., Andriolo, A., Costa, D.P., Robinson, P.W., Duffy, C.A., Nasby-Lucas, N. and Holdaway, R.N., 2017. Route fidelity during marine megafauna migration. *Frontiers in Marine Science*, p.422.

17 - Schanner, M., Bohsung, L., Fischer, C., Korte, M. and Holschneider, M., 2023. The global geomagnetic field over the historical era: what can we learn from ship-log declinations?. *Earth, Planets and Space*, *75*(1), p.96.

18 – Tormosov, D.D., “SOVALL.xls,”personal communication, via P.J. Clapham.

19 - NCEI Geomagnetic Modeling Team. 2017: Enhanced Magnetic Model 2017. NOAA National Centers for Environmental Information. Accessed [28 January, 2020]

20 - Chulliat, A., Brown, W., Alken, P., Beggan, C., Nair, M., Cox, G., Woods, A., Macmillan, S., Meyer, B. and Paniccia, M., 2020. The US/UK world magnetic model for 2020-2025.

21 - Meeus, J.H., 1991. *Astronomical algorithms*. Willmann-Bell, Incorporated.

22 - Mate, B.R., Gisiner, R. and Mobley, J., 1998. Local and migratory movements of Hawaiian humpback whales tracked by satellite telemetry. *Canadian Journal of Zoology*, *76*(5), pp.863-868.

23 - Mate, B., Mesecar, R. and Lagerquist, B., 2007. The evolution of satellite-monitored radio tags for large whales: One laboratory's experience. *Deep Sea Research Part II: Topical Studies in Oceanography*, *54*(3-4), pp.224-247.

24 - Lagerquist, B.A., Mate, B.R., Ortega-Ortiz, J.G., Winsor, M. and Urbán-Ramirez, J., 2008. Migratory movements and surfacing rates of humpback whales (*Megaptera novaeangliae*) satellite tagged at Socorro Island, Mexico. *Marine Mammal Science*, *24*(4), pp.815-830.

25 - Hauser, N., Zerbini, A.N., Geyer, Y., Heide-Jørgensen, M.P. and Clapham, P., 2010. Movements of satellite-monitored humpback whales, *Megaptera novaeangliae*, from the Cook Islands. *Marine Mammal Science*, *26*(3), pp.679-685.

26 - Garrigue, C., Clapham, P.J., Geyer, Y., Kennedy, A.S. and Zerbini, A.N., 2015. Satellite tracking reveals novel migratory patterns and the importance of seamounts for endangered South Pacific humpback whales. *Royal Society open science*, *2*(11), p.150489.

27 - Andrews-Goff, V., Bestley, S., Gales, N.J., Laverick, S.M., Paton, D., Polanowski, A.M., Schmitt, N.T. and Double, M.C., 2018. Humpback whale migrations to Antarctic summer foraging grounds through the southwest Pacific Ocean. *Scientific reports*, *8*(1), p.12333.

28 - Riekkola, L., Zerbini, A.N., Andrews, O., Andrews-Goff, V., Baker, C.S., Chandler, D., Childerhouse, S., Clapham, P., Dodémont, R., Donnelly, D. and Friedlaender, A., 2018. Application of a multi-disciplinary approach to reveal population structure and Southern Ocean feeding grounds of humpback whales. *Ecological Indicators*, *89*, pp.455-465.

29 - Modest, M., Irvine, L., Andrews-Goff, V., Gough, W., Johnston, D., Nowacek, D., Pallin, L., Read, A., Moore, R.T. and Friedlaender, A., 2021. First description of migratory behavior of humpback whales from an Antarctic feeding ground to a tropical calving ground. *Animal Biotelemetry*, *9*(1), pp.1-16.

30 - Kennedy, A.S., Zerbini, A.N., Vásquez, O.V., Gandilhon, N., Clapham, P.J. and Adam, O., 2014b. Local and migratory movements of humpback whales (*Megaptera novaeangliae*) satellite-tracked in the North Atlantic Ocean. *Canadian Journal of Zoology*, *92*(1), pp.9-18.

31 - Kettemer, L.E., Rikardsen, A.H., Biuw, M., Broms, F., Mul, E. and Blanchet, M.A., 2022. Round-trip migration and energy budget of a breeding female humpback whale in the Northeast Atlantic. *Plos one*, *17*(5), p.e0268355.

32 - Rosenbaum, H.C., Maxwell, S.M., Kershaw, F. and Mate, B., 2014. Long-range movement of humpback whales and their overlap with anthropogenic activity in the South Atlantic Ocean. *Conservation Biology*, *28*(2), pp.604-615.

33 - Zerbini, A.N., Andriolo, A., Heide-Jørgensen, M.P., Pizzorno, J.L., Maia, Y.G., VanBlaricom, G.R., DeMaster, D.P., Simões-Lopes, P.C., Moreira, S. and Bethlem, C., 2006. Satellite-monitored movements of humpback whales *Megaptera novaeangliae* in the Southwest Atlantic Ocean. *Marine Ecology Progress Series*, *313*, pp.295-304.

34 - Abrahms, B., Hazen, E.L., Aikens, E.O., Savoca, M.S., Goldbogen, J.A., Bograd, S.J., Jacox, M.G., Irvine, L.M., Palacios, D.M. and Mate, B.R., 2019. Memory and resource tracking drive blue whale migrations. *Proceedings of the National Academy of Sciences*, *116*(12), pp.5582-5587.

35 - Irvine LM, Palacios DM, Lagerquist BA, Mate BR, Follett TM. 2019. Data from: Scales of blue and fin whale feeding behavior off California, USA, with implications for prey patchiness. Movebank Data Repository. https://www.doi.org/10.5441/001/1.47h576f2

36 - Irvine, L.M., Winsor, M.H., Follett, T.M., Mate, B.R. and Palacios, D.M., 2020. An at-sea assessment of Argos location accuracy for three species of large whales, and the effect of deep-diving behavior on location error. *Animal biotelemetry*, *8*, pp.1-17.

37 - Mate BR, Palacios DM, Irvine LM, Follett TM. 2019. Data from: Behavioural estimation of blue whale movements in the Northeast Pacific from state-space model analysis of satellite tracks. Movebank Data Repository. https://www.doi.org/10.5441/001/1.5ph88fk2

38 - Hucke-Gaete, R., Bedrinana-Romano, L., Viddi, F.A., Ruiz, J.E., Torres-Florez, J.P. and Zerbini, A.N., 2018. From Chilean Patagonia to Galapagos, Ecuador: novel insights on blue whale migratory pathways along the Eastern South Pacific. *PeerJ*, *6*, p.e4695.

39 - Pérez-Jorge, S., Tobeña, M., Prieto, R., Vandeperre, F., Calmettes, B., Lehodey, P. and Silva, M.A., 2020. Environmental drivers of large-scale movements of baleen whales in the mid-North Atlantic Ocean. *Diversity and Distributions*, *26*(6), pp.683-698.

40 - Block, B.A., Jonsen, I.D., Jorgensen, S.J., Winship, A.J., Shaffer, S.A., Bograd, S.J., Hazen, E.L., Foley, D.G., Breed, G.A., Harrison, A.L. and Ganong, J.E., 2011. Tracking apex marine predator movements in a dynamic ocean. *Nature*, *475*(7354), pp.86-90.

41 - Cotté, C., d'Ovidio, F., Chaigneau, A., Lévy, M., Taupier-Letage, I., Mate, B. and Guinet, C., 2011. Scale-dependent interactions of Mediterranean whales with marine dynamics. *Limnology and Oceanography*, *56*(1), pp.219-232.

42 - Lydersen, C., Vacquié-Garcia, J., Heide-Jørgensen, M.P., Øien, N., Guinet, C. and Kovacs, K.M., 2020. Autumn movements of fin whales (*Balaenoptera physalus*) from Svalbard, Norway, revealed by satellite tracking. *Scientific reports*, *10*(1), p.16966.

43 - Silva, M.A., Prieto, R., Jonsen, I., Baumgartner, M.F. and Santos, R.S., 2013. North Atlantic blue and fin whales suspend their spring migration to forage in middle latitudes: building up energy reserves for the journey?. *PloS one*, *8*(10), p.e76507.

44 - Heide-Jørgensen, M.P., Laidre, K.L., Litovka, D., Villum Jensen, M., Grebmeier, J.M. and Sirenko, B.I., 2012. Identifying gray whale (*Eschrichtius robustus*) foraging grounds along the Chukotka Peninsula, Russia, using satellite telemetry. *Polar Biology*, *35*, pp.1035-1045.

45 - Mate, B.R., Ilyashenko, V.Y., Bradford, A.L., Vertyankin, V.V., Tsidulko, G.A., Rozhnov, V.V. and Irvine, L.M., 2015. Critically endangered western gray whales migrate to the eastern North Pacific. *Biology letters*, *11*(4), p.20150071.

46 - Williamson, J.M., 1998. WhaleNet--Interactive Education and Research Utilizing Advanced Technologies. *Marine Technology Society. Marine Technology Society Journal*, *32*(1), p.106.

47 - Mate, B.R., Nieukirk, S.L. and Kraus, S.D., 1997. Satellite-monitored movements of the northern right whale. *The Journal of wildlife management*, pp.1393-1405.

48 - Baumgartner, M.F. and Mate, B.R., 2005. Summer and fall habitat of North Atlantic right whales (*Eubalaena glacialis*) inferred from satellite telemetry. *Canadian Journal of Fisheries and Aquatic Sciences*, *62*(3), pp.527-543.

49 - Mate, B.R., Best, P.B., Lagerquist, B.A. and Winsor, M.H., 2011. Coastal, offshore, and migratory movements of South African right whales revealed by satellite telemetry. *Marine Mammal Science*, *27*(3), pp.455-476.

50 - Zerbini, A.N., Fernandez Ajos, A., Andriolo, A., Clapham, P.J., Crespo, E., Gonzalez, R., Harris, G., Mendez, M., Rosenbaum, H. and Sironi, M., 2018. Satellite tracking of Southern right whales (*Eubalaena australis*) from Golfo San Matias, Rio Negro Province, Argentina. *Scientific Committee of the International Whaling Commission SC67b, Bled, Slovenia*, *14*.

51 - Fortune, S.M., Young, B.G. and Ferguson, S.H., 2020. Age-and sex-specific movement, behaviour and habitat-use patterns of bowhead whales (*Balaena mysticetus*) in the Eastern Canadian Arctic. *Polar Biology*, *43*, pp.1725-1744.

52 - Mate, B.R., Krutzikowsky, G.K. and Winsor, M.H., 2000. Satellite-monitored movements of radio-tagged bowhead whales in the Beaufort and Chukchi seas during the late-summer feeding season and fall migration. *Canadian Journal of Zoology*, *78*(7), pp.1168-1181.

53- Alerstam, T., 2006. Conflicting evidence about long-distance animal navigation. *Science*, *313*(5788), pp.791-794.

54 - Wiltschko, R. and Wiltschko, W., 2023. Animal navigation: how animals use environmental factors to find their way. *The European Physical Journal Special Topics*, *232*(2), pp.237-252.

55 - Åkesson, S., Boström, J., Liedvogel, M. and Muheim, R., 2014. Animal navigation. *Animal movement across scales*, *21*, pp.151-178.

56 - Andreatta, G. and Tessmar-Raible, K., 2020. The still dark side of the moon: molecular mechanisms of lunar-controlled rhythms and clocks. *Journal of molecular biology*, *432*(12), pp.3525-3546.

57 - Baird, R.W., James, J., Mata, C. and Hughes, M., 2022. Two Gray Whale (*Eschrichtius robustus*) Sightings off Hawaiʻi Island: The First Records for the Central Tropical Pacific. *Aquatic Mammals*, *48*(5), pp.432-435.

58 - Hammer, Ø. and Harper, D.A., 2001. Past: paleontological statistics software package for education and data analysis. *Palaeontologia electronica*, *4*(1), p.1.

59 - Worton, B.J., 1989. Kernel methods for estimating the utilization distribution in home-range studies. *Ecology*, *70*(1), pp.164-168.

60 - Wessa, P. (2024), Free Statistics Software, Office for Research Development and Education, version 1.2.1, URL https://www.wessa.net/

61 - Woolf, B., 1957. The log likelihood ratio test (the G-test). *Annals of human genetics*, *21*(4), pp.397-409.

FIGURE LEGENDS

Fig. 1. Magnetic declination data distributions, determined by kernel density estimation, for satellite-tagged baleen whales. Colours, and the total number of once-daily platform transmitting terminal locations, as indicated in the legend.

Fig. 2. Magnetic declination data distributions, determined by kernel density estimation, for historic American and Soviet whaleship logbook entries for baleen whales (colours as indicated in the legend). The total number of 'sights and strikes' for each species are indicated in the legend.

Fig. 3. Heliologic, magnetic and heliomagnetic orientation cues available to baleen whales in the southern (A) and northern (B) magnetic hemispheres. Abbreviations and colours are as follows: SRA = sunrise azimuth (orange), positive in the clockwise direction viewed from above; SSA = sunset azimuth (red), positive in the clockwise direction viewed from above; SSA_{acw} = sunset azimuth anti-clockwise (brown), positive in the anti-clockwise direction viewed from above; SCAN = sun culmination angular altitude relative to geographic north horizon (yellow); MD = magnetic declination (light blue), positive to the east of geographic north and negative to the west of geographic north; MI = magnetic inclination (pink), positive below the geographic north horizon and negative above the geographic north horizon. GN, GE, GS, and GW indicate the geographic north, east, south and west directions, respectively. Heliomagnetic coordinates,

SRA-MD (blue) and SSA_{acw}+MD (purple), correspond with the angle in the horizontal plane between MD and SRA, and SSA_{acw}, respectively.

Fig. 4. Bivariate plot of sunset azimuth anti-clockwise plus magnetic declination (i.e., SSA_{acw}+MD) versus sunrise azimuth minus magnetic declination (i.e., SRA-MD) for historic American and Soviet whaling-ship logbook entries (brown circles) and satellite-tagged baleen whales (light blue circles).

Fig. 5. Bivariate plot of sunset azimuth anti-clockwise plus magnetic declination (i.e., SSA_{acw}+MD) versus sunrise azimuth minus magnetic declination (i.e., SRA-MD) for satellite-tagged baleen whales. Red inset box in (A) is expanded in (B). Fifteen representative individual whales, tracked via satellite, are shown in (A) and are symbolized as indicated in the legend. Symbol sizes in (A) and (B) correspond with whale movement velocity. Examples of the three heliomagnetic navigation modes (HH1-HH3), and seasonal residence (R), described in the text are indicated via arrows. All other satellite tagging data is shown as small light blue circles in (A).

Extended Data Figure 1. Magnetic declination data distributions, determined by kernel density estimation, for satellite-tagged humpback whales (solid) and historically whaled humpback whales (striped) in the Atlantic, Pacific and Indian Ocean basins (see legends for colour coding). Sample sizes indicated in the legend correspond with the total number of once-daily platform transmitting terminal whale locations (i.e., “Satellite”), and historic whaleship ‘sight or strike’ locations (i.e., “Whaling”), in each ocean basin.

Extended Data Figure 2. Magnetic declination data distributions, determined by kernel density estimation, for satellite-tagged humpback whales with major and minor modal locations, reported in Table 1, indicated (e.g., 1M = First Major Mode; 1m = First Minor Mode; 2m = Second Minor Mode; 3m = Third Minor Mode). Sample sizes indicated in the legend correspond with the total number of once-daily platform transmitting terminal whale locations.

Extended Data Figure 3. Magnetic declination data distributions, determined by kernel density estimation, for baleen whales reported in digitised whaling-ship logbooks with major and minor modal locations, reported in Table 1, indicated (e.g., 1M = First Major Mode; 1m = First Minor Mode; 2m = Second Minor Mode; 3m = Third Minor Mode). Sample sizes indicated in the legend correspond with the total number of “sight and strike” locations included in the current study.

Extended Data Figure 4. Bivariate plots of sunset azimuth anti-clockwise plus magnetic declination (i.e., SSA_{acw}+MD) versus sunrise azimuth minus magnetic declination (i.e., SRA-MD) for 17 individual baleen whales tracked via satellite-monitored platform transmitting terminal. Gray whales, recolonizing Hawai’i (A), fin whales recolonizing Elephant Island (B) and a vagrant gray whale sighted in the Atlantic Ocean (C), are shown as yellow stars.

Extended Data Figures 1-4

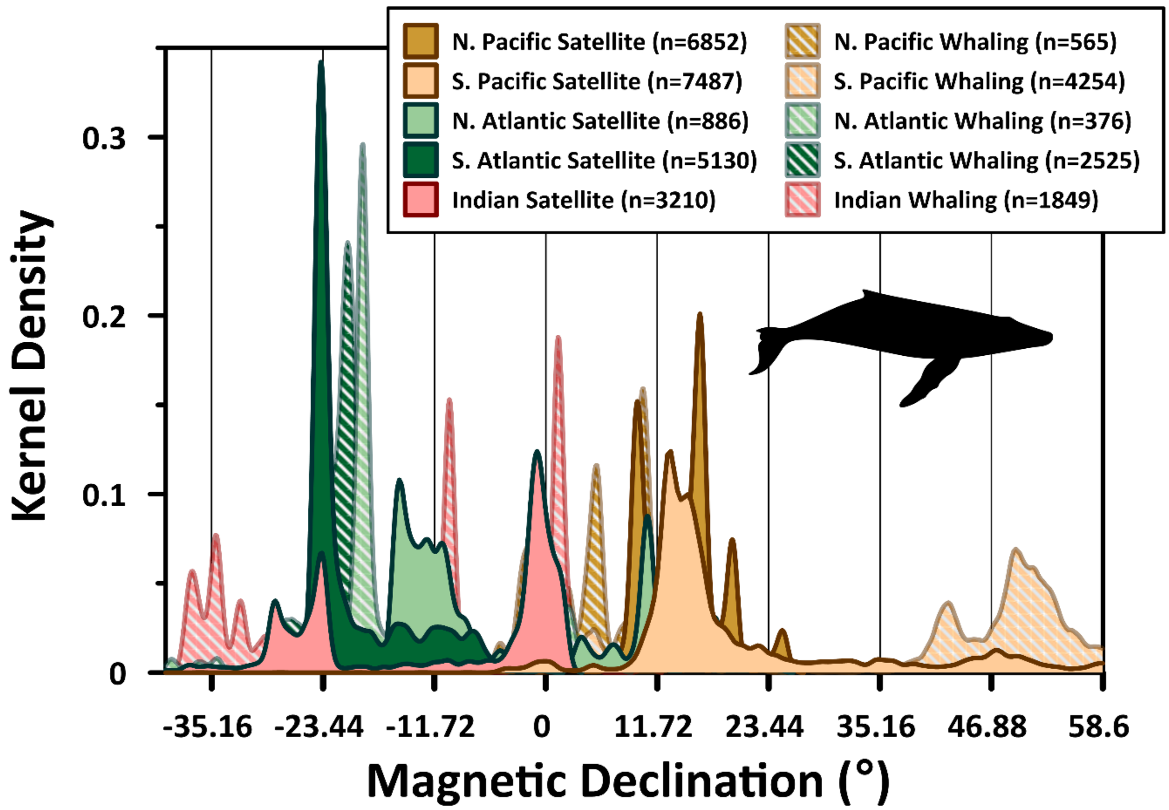

Extended Data Figure 1. Magnetic declination data distributions, determined by kernel density estimation, for satellite-tagged humpback whales (solid) and historically whaled humpback whales (striped) in the Atlantic, Pacific and Indian Ocean basins (see legends for colour coding). Sample sizes indicated in the legend correspond with the total number of once-daily platform transmitting terminal whale locations (i.e., "Satellite"), and historic whaleship 'sight or strike' locations (i.e., "Whaling"), in each ocean basin.

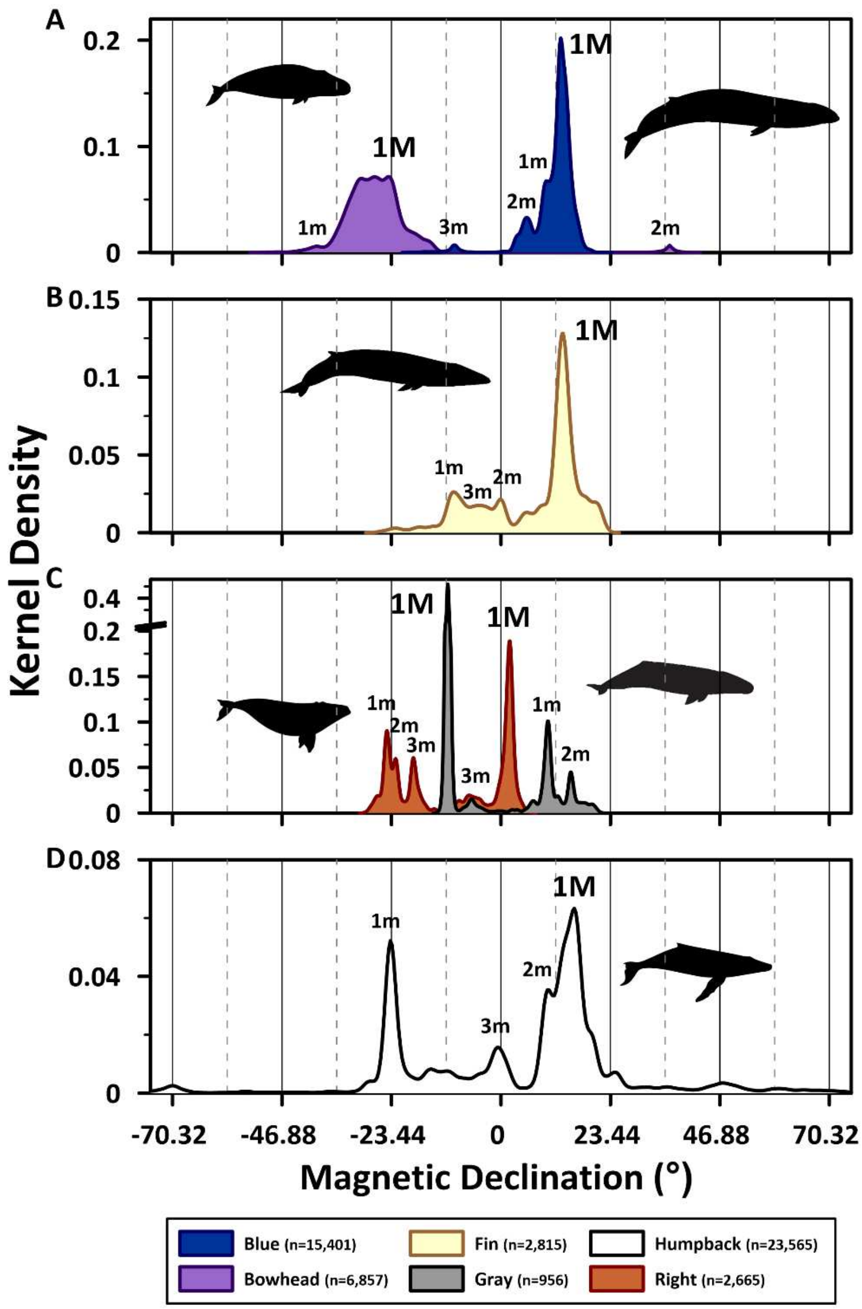

Extended Data Figure 2. Magnetic declination data distributions, determined by kernel density estimation, for satellite-tagged humpback whales with major and minor modal locations, reported in Table 1, indicated (e.g., 1M = First Major Mode; 1m = First Minor Mode; 2m = Second Minor Mode; 3m = Third Minor Mode). Sample sizes indicated in the legend correspond with the total number of once-daily platform transmitting terminal whale locations.

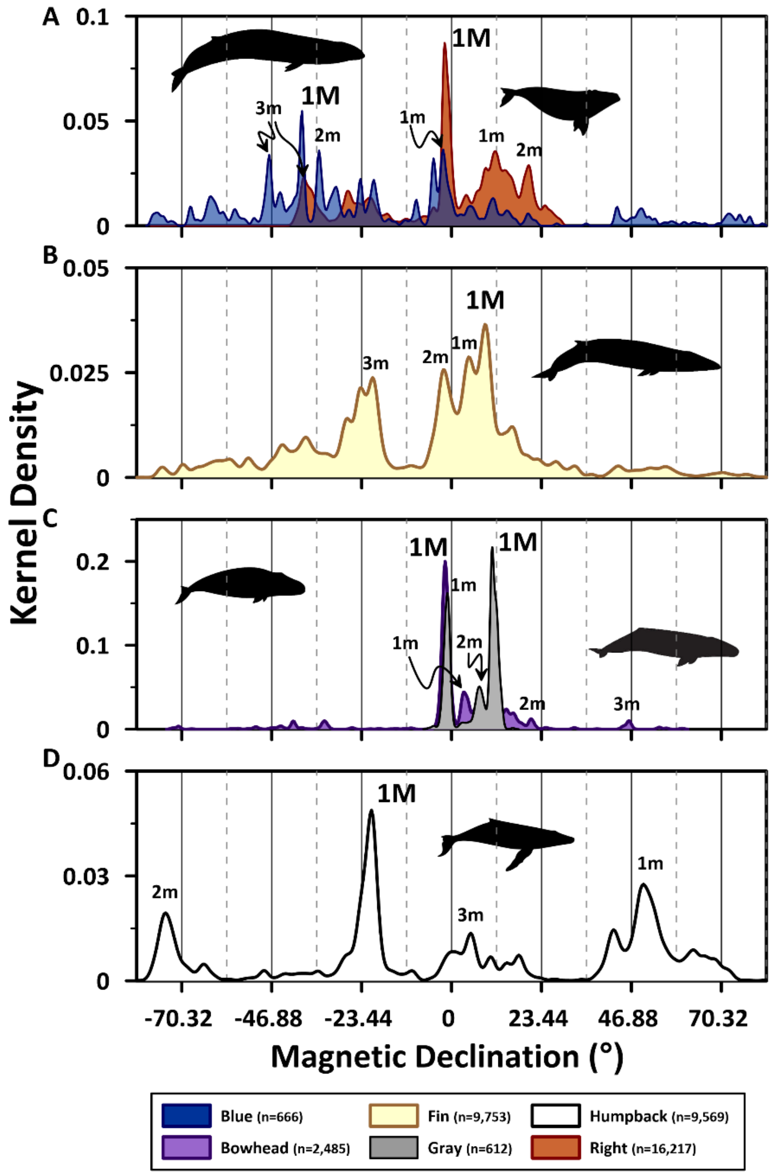

Extended Data Figure 3. Magnetic declination data distributions, determined by kernel density estimation, for baleen whales reported in digitised whaling-ship logbooks with major and minor modal locations, reported in Table 1, indicated (e.g., 1M = First Major Mode; 1m = First Minor Mode; 2m = Second Minor Mode; 3m = Third Minor Mode). Sample sizes indicated in the legend correspond with the total number of "sight and strike" locations included in the current study.

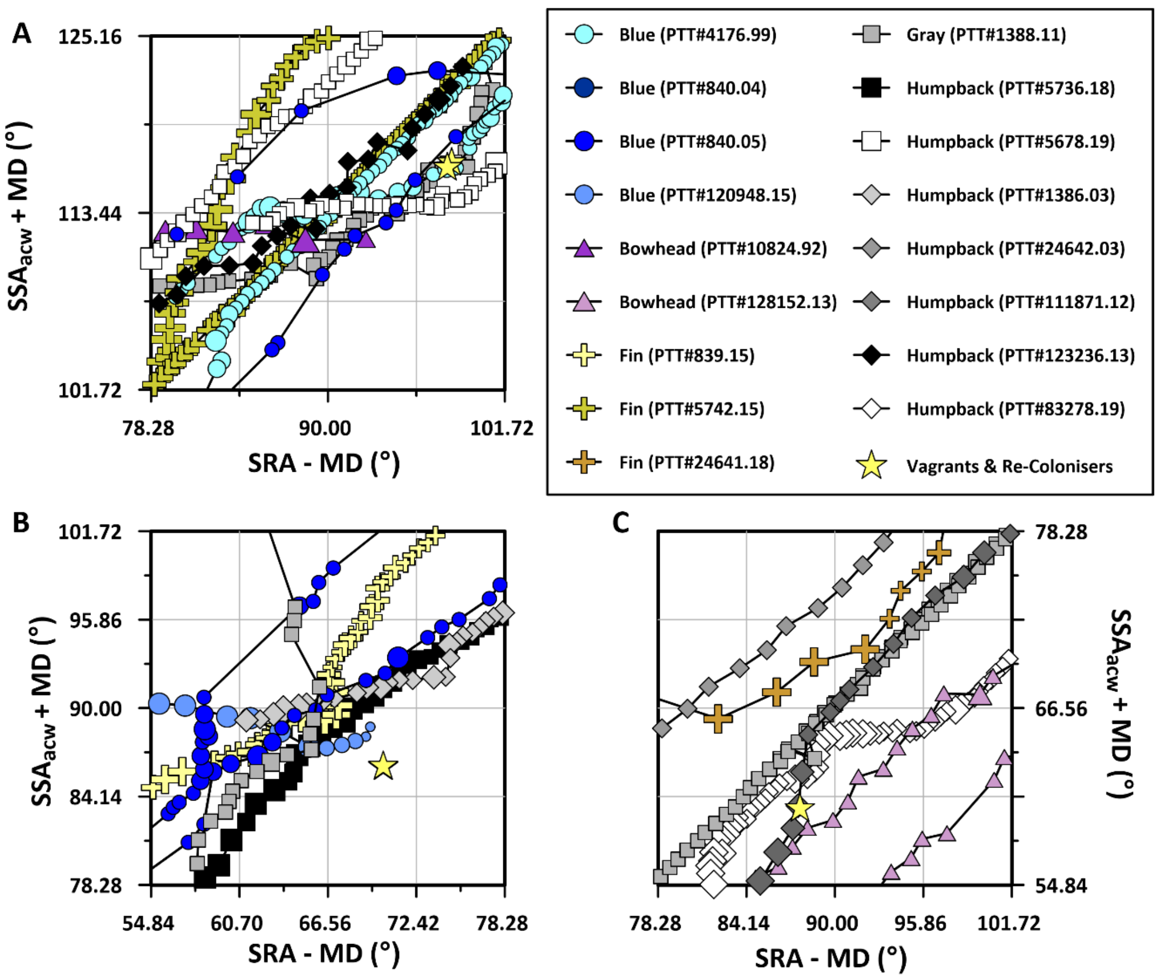

Extended Data Figure 4. Bivariate plots of sunset azimuth anti-clockwise plus magnetic declination (i.e., SSA_{acw}+MD) versus sunrise azimuth minus magnetic declination (i.e., SRA-MD) for 17 individual baleen whales tracked via satellite-monitored platform transmitting terminal. Gray whales, recolonizing Hawai'i (A), fin whales recolonizing Elephant Island (B) and a vagrant gray whale sighted in the Atlantic Ocean (C), are shown as yellow stars.

Supplementary Files

This is a list of supplementary files associated with this preprint. Click to download.

- TableS1.xlsx
- TableS2.xlsx